

## Anharmonic double-phonon excitations in the interacting boson model

J. E. García-Ramos,<sup>1,2</sup> J. M. Arias,<sup>2</sup> and P. Van Isacker<sup>3</sup>

<sup>1</sup>*Institute for Theoretical Physics, Vakgroep Subatomaire en Stralingsfysica, Proeftuinstraat 86, B-9000 Gent, Belgium*

<sup>2</sup>*Departamento de Física Atómica, Molecular y Nuclear, Universidad de Sevilla, Aptdo. 1065, E-41080 Sevilla, Spain*

<sup>3</sup>*Grand Accélérateur National d'Ions Lourds, B.P. 5027, F-14076 Caen Cedex 5, France*

(Received 12 July 2000; published 14 November 2000)

Double- $\gamma$  vibrations in deformed nuclei are analyzed in the context of the interacting boson model. A simple extension of the original version of the model towards higher-order interactions is required to explain the observed anharmonicities of nuclear vibrations. The influence of three- and four-body interactions on the moments of inertia of ground and  $\gamma$  bands, and on the relative position of single- $\gamma$  and double- $\gamma$  bands is studied in detail. As an example of a realistic calculation, spectra and transitions of the highly  $\gamma$ -anharmonic nuclei  $^{164}\text{Dy}$ ,  $^{166}\text{Er}$ , and  $^{168}\text{Er}$  are interpreted in this approach.

PACS number(s): 21.60.Fw, 21.60.Ev, 21.10.Re, 27.70.+q

### I. INTRODUCTION

Vibrational degrees of freedom in atomic nuclei can be described in terms of phonon excitations that arise from nuclear shape oscillations. Vibrations of nuclei with ellipsoidal symmetry can be of two types [1]:  $\beta$  vibrations which preserve axial symmetry and give rise to a band with  $K=0$ , and  $\gamma$  vibrations which break axial symmetry and yield a  $K=2$  band, where  $K$  is the projection of the angular momentum on the axis of symmetry. At the experimental level,  $\gamma$  bands have been identified in many well-deformed nuclei; in contrast, the identification of  $\beta$  bands is still full of questions and difficulties. This is mainly because, when the energy surface has a well-deformed minimum in  $\beta$  but is rather flat in  $\gamma$ , the  $\beta$  band increases in excitation energy and approaches the energy region where other degrees of freedom are important. In that case band mixing may occur and can give rise to nonpure structures with decay patterns difficult to identify as those of a  $\beta$  band [2].

Since single- $\gamma$  excitations are very well established, it is natural to look for double- $\gamma$  vibrations and to develop models that can deal with such multiphonon excitations. Double- $\gamma$  excitations correspond to  $K^\pi=0^+$  and  $K^\pi=4^+$  bands which are the antiparallel and parallel combinations of single- $\gamma$  phonons, respectively. The experimental identification of two- $\gamma$  states in deformed nuclei is difficult because their expected excitation energy is around the pairing gap and hence they can mix strongly with two-quasiparticle excitations. However, recent experimental improvements in nuclear spectroscopy following Coulomb excitation [3], inelastic neutron scattering [4], and thermal-neutron capture [5] have made possible the study of highly excited low-spin states. Many states have been proposed as possible candidates of double- $\gamma$  vibrations. There is, however, some controversy about their interpretation. The author of Ref. [6] claims that some of the presumed double- $\gamma$  states can be interpreted as single hexadecapole-phonon excitations. In fact, to identify the band head of a double- $\gamma$  band it is not sufficient to analyze just  $B(E2)$  values; data from single-nucleon transfer reactions,  $\beta$ -decay studies, and inelastic

scattering experiments must be considered as well. One of the key properties to disregard a band as a double- $\gamma$  band is the fact that its members, in first order, cannot be populated in single-nucleon transfer reactions. Many examples of  $K^\pi=4^+$  states that are identified as double- $\gamma$  excitations but are strongly populated in single-nucleon transfer reactions, can be found in the literature:  $^{158}\text{Gd}$ ,  $^{162}\text{Dy}$ ,  $^{172}\text{Yb}$ ,  $^{176,178}\text{Hf}$ , and  $^{190,192}\text{Os}$ . Since the double-phonon character of the states in question is in doubt, they are not considered here. However, some candidates seem to have a genuine double-phonon nature. Such is the case with  $^{164}\text{Dy}$  and  $^{166-68}\text{Er}$ . In particular, in Ref. [7] a  $K^\pi=4^+$  state in  $^{164}\text{Dy}$  at 2.173 MeV is found to exhibit all properties of a double- $\gamma$  band. In Refs. [8] and [9] the observation is reported of  $K^\pi=0^+$  and  $K^\pi=4^+$  double- $\gamma$  states in  $^{166}\text{Er}$ , at energies of 1.949 and 2.029 MeV, respectively. Finally, in  $^{168}\text{Er}$  a  $K^\pi=4^+$  double- $\gamma$  excitation is identified at an energy of 2.055 MeV [10].

One of the most striking features of the observed double- $\gamma$  bands is their high anharmonicity, i.e., the ratio of double- $\gamma$  over single- $\gamma$  energy is different from 2 and ranges from 2.5 to 2.8. This information is very important since it provides a stringent test of nuclear models. The nuclei  $^{164}\text{Dy}$  and  $^{166,168}\text{Er}$  have been interpreted in the context of many different models such as the quasiphonon model [11,12], the geometrical model [13], the multiphonon model [14], the self-consistent collective-coordinate method [15,16], and the *sdg* interacting boson model (IBM) [17,18], and it is now of interest to revisit these models in connection with anharmonic vibrational behavior.

In this paper the simplest version of the interacting boson model (IBM) [19] is extended by adding to the usual Hamiltonian higher-order interactions between the bosons with the purpose of creating a framework that accommodates the high anharmonicities observed in  $^{164}\text{Dy}$  and  $^{166,168}\text{Er}$ . The structure of the paper is as follows. First, the IBM is reviewed with special reference to its harmonic character. In Sec. III the inclusion of three-body terms in the Hamiltonian is discussed. The introduction of four-body terms is presented in Sec. IV and some analytic results are pointed out. In Sec. V a detailed study of possible four-body terms is carried out

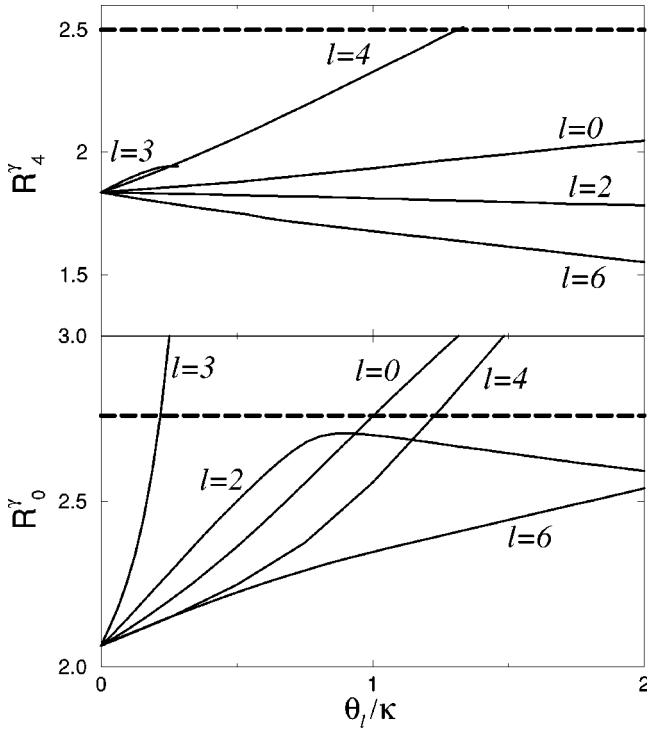


FIG. 1. The ratios  $R_k^\gamma$  (as defined in the text) as a function of  $\theta_l/\kappa$  for different  $l$ . The Hamiltonian (9) is used with  $\chi = -0.5$ ; the boson number is  $N = 15$ . The dashed lines give the experimental values for the corresponding ratios in  $^{166}\text{Er}$ .

and realistic calculations for  $^{164}\text{Dy}$  and  $^{166,168}\text{Er}$  are presented. Finally, in Sec. VI the conclusions of this work are made.

## II. THE IBM-1 AS A HARMONIC MODEL

The IBM describes low-lying collective excitations in even-even nuclei in terms of monopole ( $s$ ) and quadrupole

( $d$ ) bosons [19]. The boson number that corresponds to a given nucleus equals half the number of valence nucleons ( $N = n/2$ ). The rotationally invariant and number-conserving boson Hamiltonian usually includes up to two-body interactions between the bosons although higher-order terms can be added in principle. The most general two-body IBM Hamiltonian can be written in a multipole expansion [19] as

$$\hat{H} = \varepsilon_s \hat{n}_s + \varepsilon_d \hat{n}_d + \kappa_0 \hat{P}^\dagger \hat{P} + \kappa_1 \hat{L} \cdot \hat{L} + \kappa_2 \hat{Q} \cdot \hat{Q} + \kappa_3 \hat{T}_3 \cdot \hat{T}_3 + \kappa_4 \hat{T}_4 \cdot \hat{T}_4, \quad (1)$$

where  $\hat{n}_s$  and  $\hat{n}_d$  are the  $s$ - and  $d$ -boson number operators, respectively, and

$$\hat{P}^\dagger = \frac{1}{2} d^\dagger \cdot d^\dagger - \frac{1}{2} s^\dagger \cdot s^\dagger, \quad (2)$$

$$\hat{L} = \sqrt{10} (d^\dagger \times \tilde{d})^{(1)}, \quad (3)$$

$$\hat{Q} = s^\dagger \tilde{d} + d^\dagger \tilde{s} + \chi (d^\dagger \times \tilde{d})^{(2)}, \quad (4)$$

$$\hat{T}_3 = (d^\dagger \times \tilde{d})^{(3)}, \quad (5)$$

$$\hat{T}_4 = (d^\dagger \times \tilde{d})^{(3)}. \quad (6)$$

The symbol “ $\cdot$ ” represents the scalar product; in this paper the scalar product of two operators with angular momentum  $L$  is defined as  $\hat{T}_L \cdot \hat{T}_L = \sum_M (-1)^M \hat{T}_{LM} \hat{T}_{L-M}$  where  $\hat{T}_{LM}$  corresponds to the  $M$  component of the operator  $\hat{T}_L$ . In the previous equations the operator  $\tilde{\gamma}_{lm} = (-1)^m \gamma_{l-m}$  (where  $\gamma$  refers to  $s$  or  $d$ ) is introduced so that the annihilation operator verifies the appropriate properties under spatial rotations.

It is not *a priori* clear to what extent  $\beta$  and  $\gamma$  vibrations are anharmonic in the IBM even if one just considers the Hamiltonian (1) with up to two-body interactions. A partial

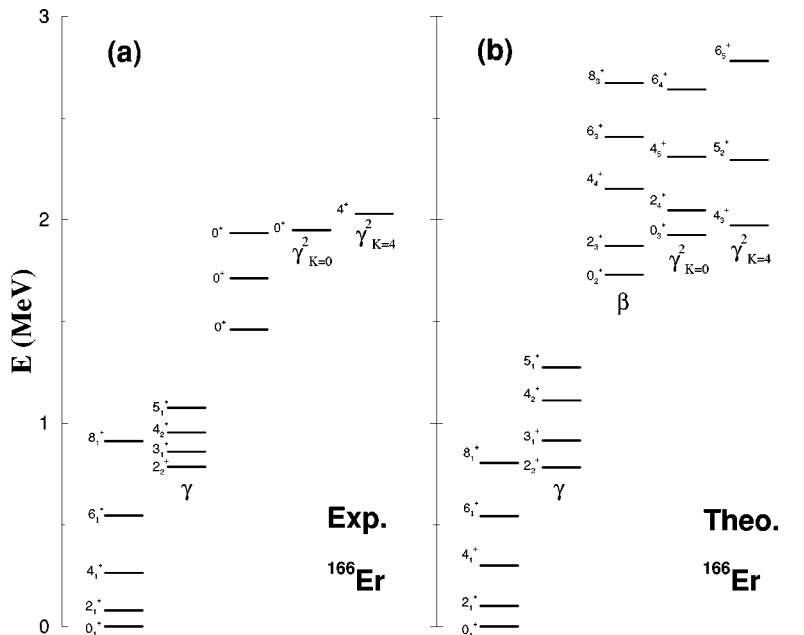


FIG. 2. Experimental (a) and calculated (b) spectrum for  $^{166}\text{Er}$ . The theoretical results are obtained with the Hamiltonian (9) with  $\kappa = 23.8$  keV,  $\chi = -0.55$ ,  $\kappa' = -1.9$  keV, and  $\theta_4 = 31.3$  keV. The boson number is  $N = 15$ .

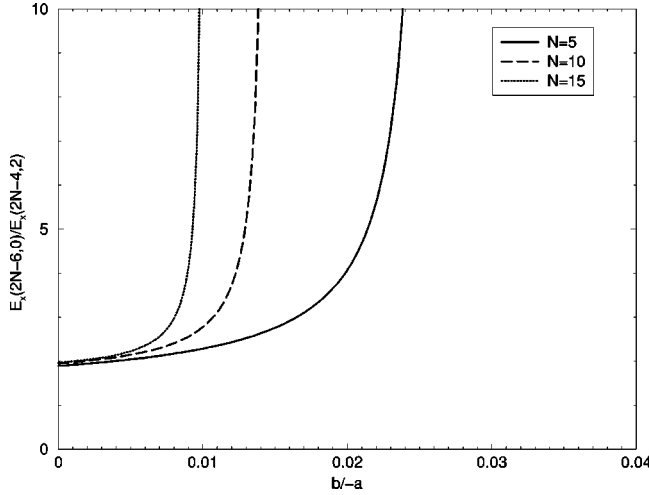


FIG. 3. The ratio  $R_0^{\text{SU}(3)\gamma}$  (as defined in the text) for the Hamiltonian  $\hat{H} = a\hat{C}_2[\text{SU}(3)] + b\hat{C}_3[\text{SU}(3)]$  with  $N=5, 10$ , and  $15$ .

analysis of this problem was given in Ref. [20]. There, the authors find that the IBM in its simplest version is a harmonic model in the limit of infinite boson number  $N$  and even for finite  $N$  the model cannot accommodate large anharmonicity if one considers up to two-body interactions; only the interplay between one+two-body terms and higher-order interactions can induce, in principle, a sizable anharmonicity in the double-phonon excitations. The reason why one-body terms and two-body interactions cannot create a large anharmonicity can be understood as follows. If one considers a Hamiltonian with one parameter that controls the ratio of the strength of the one-body energies and the two-body interactions,

$$\hat{H} = (1 - \xi)(\varepsilon_s \hat{n}_s + \varepsilon_d \hat{n}_d) + \xi(\kappa_0 \hat{P}^\dagger \hat{P} + \kappa_1 \hat{L} \cdot \hat{L} + \kappa_2 \hat{Q} \cdot \hat{Q} + \kappa_3 \hat{T}_3 \cdot \hat{T}_3 + \kappa_4 \hat{T}_4 \cdot \hat{T}_4), \quad (7)$$

where  $\xi$  ranges from 0 to 1, one finds two ‘‘phases’’ separated by a critical value,  $\xi_c$ : a first phase where the one-body term plays the main role ( $\xi < \xi_c$ ) and a second phase where the two-body interaction is the driving force ( $\xi > \xi_c$ ). The crucial point is that the separation between the two phases is very sharp [21] and essentially no interplay between one- and two-body terms can be found. Since, to a good approximation, the force is either one body or two body but not both, harmonic behavior cannot be avoided.

The inclusion of high-order interactions in a system with a high boson number also leads to a harmonic description. Only for finite boson number the interplay between one + two-body terms and higher-order interactions can induce an anharmonicity in the double-phonon excitations that is comparable to the observed one. These ideas will be used as a guideline in the following sections.

To carry out a quantitative study of anharmonicities, it is convenient to define a ratio between single- and double-phonon excitation energies. Because the experimental situation for  $\beta$  excitations is not clear we concentrate on  $\gamma$  vibra-

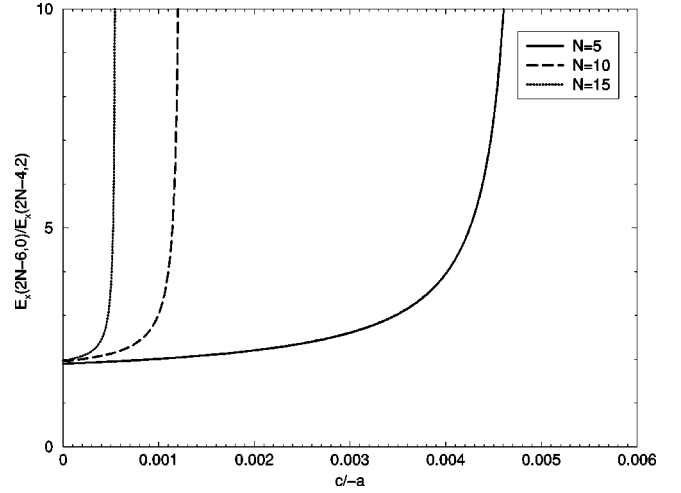


FIG. 4. The ratio  $R_0^{\text{SU}(3)\gamma}$  (as defined in the text) for the Hamiltonian  $\hat{H} = a\hat{C}_3[\text{SU}(3)] + c\hat{C}_2[\text{SU}(3)]^2$  with  $N=5, 10$ , and  $15$ .

tions and define energy ratios for  $\gamma$  phonons only (although similar definitions can be given for  $\beta$  phonons):

$$R_0^\gamma \equiv \frac{E_x(0_{\gamma\gamma}^+)}{E_x(2_\gamma^+) - E_x(2_1^+)}, \quad R_4^\gamma \equiv \frac{E_x(4_{\gamma\gamma}^+) - E_x(4_1^+)}{E_x(2_\gamma^+) - E_x(2_1^+)}, \quad (8)$$

where  $0_{\gamma\gamma}^+$  and  $4_{\gamma\gamma}^+$  are the band heads of the  $K^\pi = 0^+$  and  $K^\pi = 4^+$  double- $\gamma$  bands, respectively, and  $E_x$  stands for excitation energy. This particular definition removes any rotational influence.

### III. THREE-BODY HAMILTONIANS

Let us consider in the following a Hamiltonian that includes a quadrupole term, a rotational  $\hat{L}^2$  term, and three-body interactions between the  $d$  bosons,

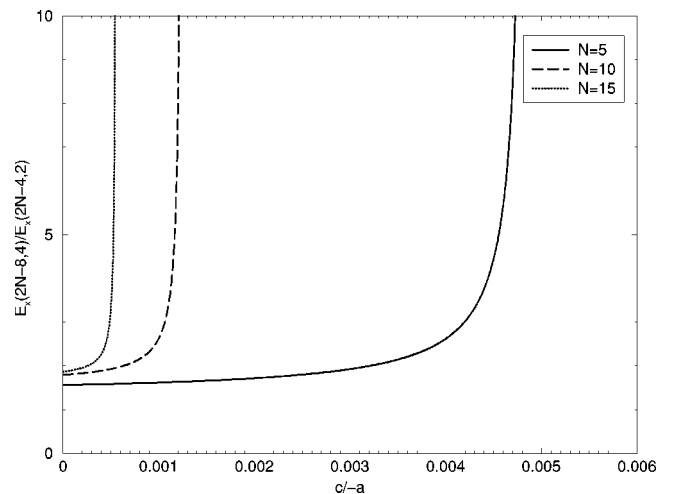


FIG. 5. The ratio  $R_4^{\text{SU}(3)\gamma}$  (as defined in the text) for the Hamiltonian  $\hat{H} = a\hat{C}_2[\text{SU}(3)] + c\hat{C}_2[\text{SU}(3)]^2$  with  $N=5, 10$ , and  $15$ .

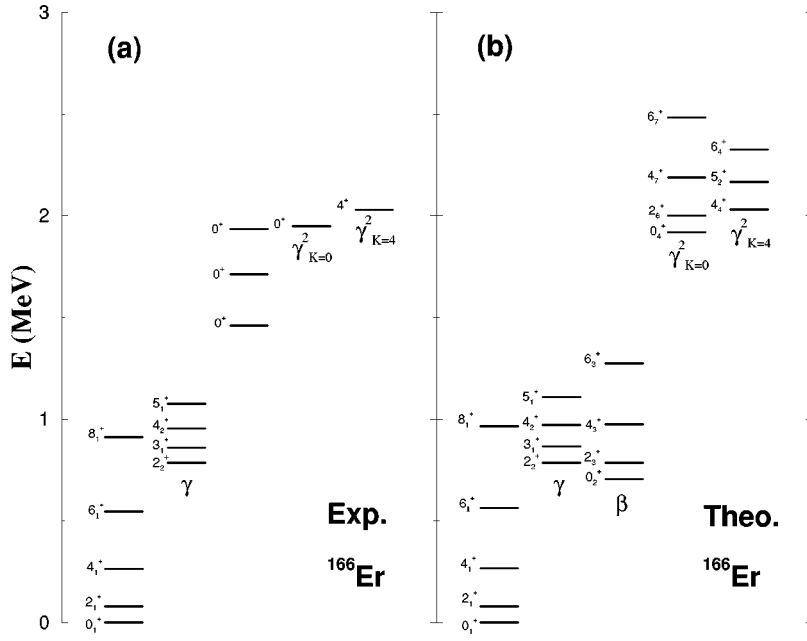


FIG. 6. Experimental (a) and theoretical (b) spectrum for  $^{166}\text{Er}$ . The theoretical results are obtained with the Hamiltonian  $\hat{H} = 13.43\hat{L}^2 - 20.84\hat{C}_2[\text{SU}(3)] + 9.296 \times 10^{-3}\hat{C}_2[\text{SU}(3)]^2$  (all coefficients in keV) with  $\chi = -\sqrt{7}/2$ . The boson number is  $N = 15$ .

$$\hat{H} = -\kappa\hat{Q} \cdot \hat{Q} + \kappa'\hat{L} \cdot \hat{L} + \sum_{kl} \theta_l [(d^\dagger \times d^\dagger)^{(k)} \times d^\dagger]^{(l)} \cdot [(\tilde{d} \times \tilde{d})^{(k)} \times \tilde{d}]^{(l)}, \quad (9)$$

where  $-\kappa = \kappa_2$ ,  $\kappa' = \kappa_1$ . Five independent three-body  $d$ -boson interactions exist which have  $l = 0, 2, 3, 4$ , and  $6$ . Interactions with the same  $l$  but different  $k$  are not independent but differ by a normalization factor only [22]. The combinations  $(k, l) = (2, 0), (0, 2), (2, 3), (2, 4)$ , and  $(4, 6)$  are chosen here.

The Hamiltonian (9) is certainly not the most general one +two+three-body Hamiltonian that can be considered. Notably, a vibrational term  $\epsilon_d \hat{n}_d$  which dominates in spherical nuclei is omitted since it is thought of lesser importance in the deformed nuclei considered here. And, of all possible three-body interactions (seventeen terms), only those between the  $d$  bosons are retained here since they are the more efficient terms to produce anharmonicity [23].

For the discussion of the anharmonicities of  $\gamma$  vibrations we study the behavior of the energy ratios (8) as a function of the ratio  $\theta_l/\kappa$ . The identification of the states  $0_{\gamma\gamma}^+$  and  $4_{\gamma\gamma}^+$  is based on the  $B(E2)$  values for decay into the single- $\gamma$  states. In Fig. 1,<sup>1</sup> the influence of the various three-body interactions is shown for a typical value of  $\chi$  ( $\chi = -0.5$ ) and for  $N = 15$  bosons. It is seen that a  $\gamma$ -vibrational anharmonic behavior is obtained which can be different for the  $K^\pi = 0^+$  and  $K^\pi = 4^+$  bands (e.g., positive for the former while negative for the latter). Care has been taken to plot results only up to values of  $\theta_l$  that do not drastically alter the character of rotational spectrum; beyond these values, the three-body interaction, being of highest order in the Hamiltonian

(9), becomes dominant. Also shown in Fig. 1 are the ratios  $R_K^\chi$  as observed in  $^{166}\text{Er}$  [8,9],  $R_0^\gamma = 2.76$  and  $R_4^\gamma = 2.50$ . Figure 2 shows the experimental spectrum of  $^{166}\text{Er}$  [8,9] and compares it to the eigenspectrum of Hamiltonian (9) with an  $l = 4$  three-body interaction. The parameters are  $\kappa = 23.8$  keV,  $\chi = -0.55$ ,  $\kappa' = -1.9$  keV, and  $\theta_4 = 31.3$  keV,<sup>2</sup> with boson number  $N = 15$ . With these values the calculated excitation energies of the double- $\gamma$  band heads are 1926 keV and 1972 keV for the  $K^\pi = 0^+$  and  $K^\pi = 4^+$  levels, respectively, leading to the ratios  $R_0^\gamma = 2.82$  and  $R_4^\gamma = 2.45$ , in excellent agreement with observation. Note, however, that although all  $\gamma$ -band heads are well reproduced by the calculation, problems arise for the moments of inertia, in particular of the  $\gamma$  band. In next sections we will come back to the moments of inertia to see that three-body Hamiltonians provide a very poor description of them.

#### IV. SU(3) HAMILTONIANS WITH UP TO FOUR-BODY INTERACTIONS

In the previous section and in Ref. [24] a very good description of double-phonon excitation energy has been obtained, but at expense of spoiling the moments of inertia of ground and  $\gamma$  bands. These drawbacks seem to be a general feature of three-body Hamiltonians. In this and the following section it is shown that the drawbacks of three-body interactions can be overcome by going to the next order.

Since  $\gamma$  anharmonicity has been observed exclusively in well-deformed nuclei, it is appropriate to consider the problem in the SU(3) limit of the IBM which is suited to deal with nuclei in this mass region [25]. Therefore, in a first

<sup>1</sup>Note that this figure differs from Fig. 2 in Ref. [24] in some scale factors due to an error in the definition of  $\theta_l$ .

<sup>2</sup>Note that the value  $\theta_4$  is 1/3 of that given in Ref. [24] which has an error in its definition. The results shown in that paper are correct after a simple rescaling of the parameter.

TABLE I. Observed and calculated  $B(E2)$  values and ratios for  $^{166}\text{Er}$  in a schematic calculation using an SU(3) Hamiltonian. The  $E2$  operator (22) is used with  $e_{\text{eff}}^2 = (1.97)^2$  W.u. and  $\chi = -0.26$ .

	$B(E2)$ value or ratio	
	Observed	Calculated
$B(E2; 2_1^+ \rightarrow 0_1^+)$ (W.u.)	$214 \pm 10^a$	214
$B(E2; 4_1^+ \rightarrow 2_1^+)$ (W.u.)	$311 \pm 10^a$	302
$B(E2; 2_\gamma^+ \rightarrow 0_1^+)$ (W.u.)	$5.5 \pm 0.4^a$	5.4
$B(E2; 0_{\gamma\gamma}^+ \rightarrow 2_\gamma^+)$	$3.8 \pm 1.3^b$ ( $2.2_{-0.7}^{+1.1}$ ) <sup>c</sup>	2.5
$B(E2; 4_{\gamma\gamma}^+ \rightarrow 2_\gamma^+)$	$1.3 \pm 0.4^b$ ( $0.9 \pm 0.3^c$ )	2.5
$B(E2; 2_\gamma^+ \rightarrow 0_1^+)$		

<sup>a</sup>From Ref. [30].

<sup>b</sup>From Ref. [9].

<sup>c</sup>From Ref. [8].

approach, the SU(3) limit is used and later, in the next section, these results are used as a guidance in more realistic calculations.

Let us consider the following Hamiltonian:

$$\hat{H} = a\hat{C}_2[\text{SU}(3)] + b_1\hat{C}_3[\text{SU}(3)] + b_2\hat{N}\hat{C}_2[\text{SU}(3)] + c_1\hat{C}_2[\text{SU}(3)]^2 + c_2\hat{N}\hat{C}_3[\text{SU}(3)] + c_3\hat{N}^2\hat{C}_2[\text{SU}(3)], \quad (10)$$

where  $\hat{C}_n[\text{SU}(3)]$  stands for the Casimir operator of order  $n$  of SU(3). Note the inclusion of cubic terms for completeness in the SU(3) analysis. Since only the spectrum of a single nucleus is of interest here, the number of bosons can be fixed in every case and the Hamiltonian (10) can be sim-

plified by combining terms into a single one, leaving a Hamiltonian with three coefficients  $a$ ,  $b$ , and  $c$ ,

$$\hat{H} = a\hat{C}_2[\text{SU}(3)] + b\hat{C}_3[\text{SU}(3)] + c\hat{C}_2[\text{SU}(3)]^2, \quad (11)$$

with eigenvalues

$$\langle (\lambda, \mu) | \hat{H} | (\lambda, \mu) \rangle = a(\lambda^2 + \mu^2 + \lambda\mu + 3\lambda + 3\mu) + b(\lambda - \mu) \times (2\lambda + \mu + 3)(\lambda + 2\mu + 3) + c(\lambda^2 + \mu^2 + \lambda\mu + 3\lambda + 3\mu)^2. \quad (12)$$

No quartic Casimir operator exists for SU(3) because the number of independent Casimir operators equals the number of labels that characterize an irreducible representation. The Hamiltonian (11) has no rotational term  $\hat{L}^2$  since of primary interest, at this point, is the description of band-head energies of single- and double- $\gamma$  excitations. Note that Hamiltonian (11) is not in normal order, as a consequence, first term contains up to two-body interactions (one- and two-body), second term up to three-body interactions (one-, two-, and three-body) and third term up to four-body interactions (one-, two-, three-, and four-body).

The definition of the energy ratios (8) must now be adapted to incorporate the symmetry labeling of the states. In the SU(3) limit the  $\gamma$  band belongs to the SU(3) representation  $(2N-4, 2)$  where  $N$  is the number of bosons. The double- $\gamma$  band with  $K=4$  is contained in the  $(2N-8, 4)$  representation; the double- $\gamma$  band with  $K=0$  is predominantly contained in the  $(2N-6, 0)$  representation, although an important component is in  $(2N-8, 4)$  [20]. In this section the energy ratios (8) are thus defined as follows:

$$R_0^{\text{SU}(3)\gamma} \equiv \frac{E_x(2N-6, 0)}{E_x(2N-4, 2)}, \quad R_4^{\text{SU}(3)\gamma} \equiv \frac{E_x(2N-8, 4)}{E_x(2N-4, 2)}. \quad (13)$$

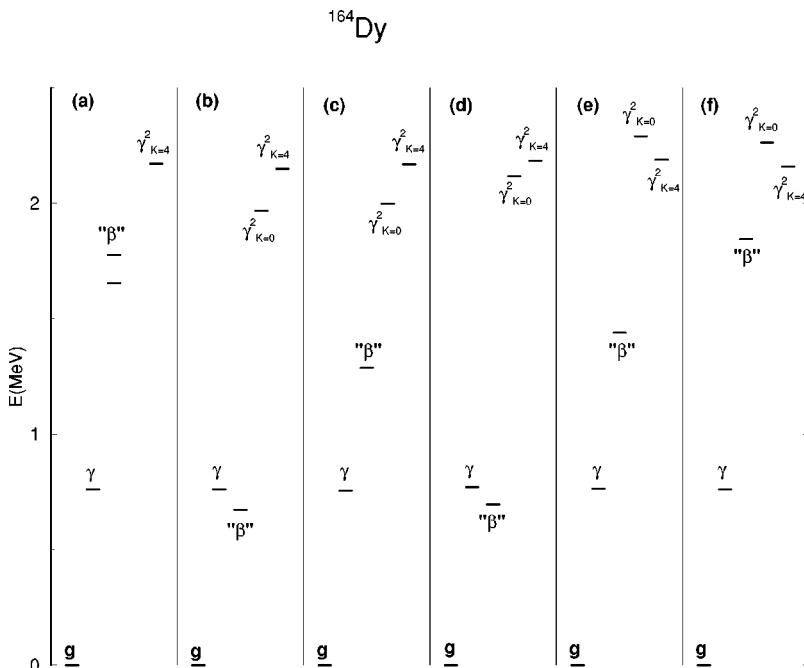


FIG. 7. Band heads of ground,  $\gamma$ ,  $\beta$ , double- $\gamma K=0$ , and double- $\gamma K=4$  bands of  $^{164}\text{Dy}$ . Panels correspond to (a) experimental data, (b) calculation with Hamiltonian (23) and  $\chi = -\sqrt{7}/2$ , (c) calculation with Hamiltonian (23) and  $\chi = -0.55$ , (d) calculation with Hamiltonian (24) and  $\chi = -\sqrt{7}/2$ , (e) calculation with Hamiltonian (24) and  $\chi = -0.55$ , and (f) calculation with Hamiltonian (9).



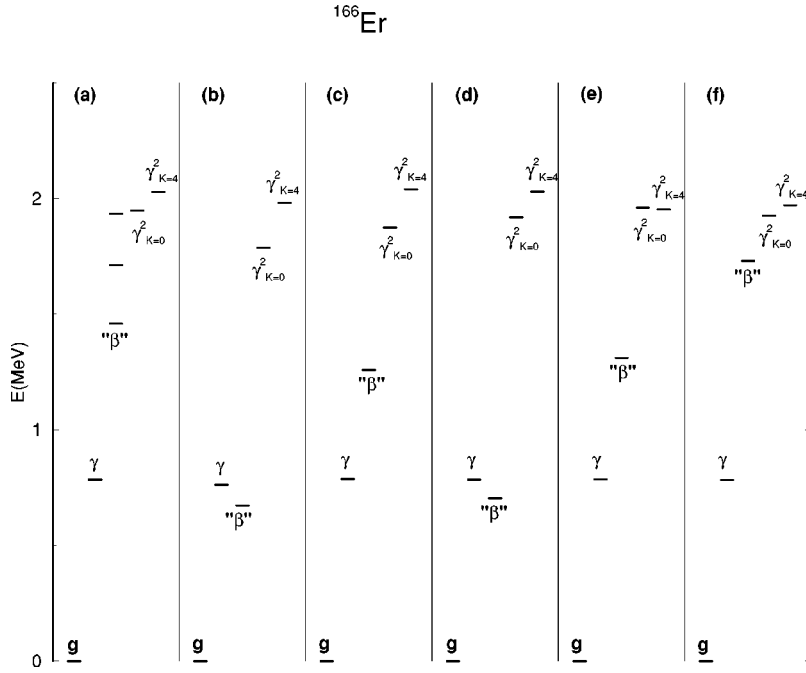


FIG. 8. Band heads of  $^{166}\text{Er}$ . See caption of Fig. 7.

Because no rotational term is included, the ratios (13) can be compared directly with Eq. (8). In the following the effect of the different terms in Eq. (11) on the degree of anharmonicity of the two-phonon excitation energy is analyzed.

(i)  $a < 0$ ,  $b = 0$ ,  $c = 0$ .

This corresponds to the simplest version of IBM; the energy ratios become

$$R_0^{\text{SU}(3)\gamma} = \frac{24N-18}{12N-6}, \quad R_4^{\text{SU}(3)\gamma} = \frac{24N-36}{12N-6}. \quad (14)$$

An almost pure harmonic  $\gamma$ -vibrational spectrum is found since the energy ratios (14) are only slightly lower than 2. This will be referred to as negative anharmonicity as opposed to the positive anharmonicity for energy ratios above 2.

(ii)  $a < 0$ ,  $b \neq 0$ ,  $c = 0$ .

In this case the Hamiltonian (11) is a combination of the quadratic and cubic  $\text{SU}(3)$  Casimir operators. For given values of  $a$  and  $b$  and for a high enough boson number, only the three-body part of the Hamiltonian is dominant and a harmonic spectrum is recovered. For obtaining an anharmonic spectrum the values of the Hamiltonian parameters are very constrained once the number of bosons has been fixed, as the following analysis shows.

Without loss of generality  $a$  can be fixed to  $a = -1$ . The energy ratios are then

$$R_0^{\text{SU}(3)\gamma} = \frac{3-4N+b(24N^2-36N+27)}{(2N-1)(6bN+9b-1)}, \quad (15)$$

$$R_4^{\text{SU}(3)\gamma} = 2\frac{2N-3}{2N-1}. \quad (16)$$

To keep the energy of the  $\gamma$  excitation positive, the value of  $b$  has an upper limit

$$b < \frac{1}{6N+9}. \quad (17)$$

The value  $b = 1/(6N+9)$  leads to a divergence in  $R_0^{\text{SU}(3)\gamma}$  and around this value anharmonic behavior is found. From Eq. (15) one observes that the behavior of the  $(2N-8,4)$  representation is completely harmonic and does not depend on  $b$ . On the other hand, from Eq. (15) one sees that a wide range of anharmonic ratios is found for the  $(2N-6,0)$  representation. As an illustration, in Fig. 3 Eq. (15) is represented as a function of  $b$ , for three values of  $N$  (5, 10, and 15). Only positive values of  $b$  are plotted because for the negative ones  $R_0^{\text{SU}(3)\gamma}$  decreases smoothly to the asymptotic values 1.27, 1.58, and 1.70 for  $N=5$ , 10, and 15, respectively.

The conclusion is that a Hamiltonian with  $c=0$  does not agree with the experimental situation observed in the mass region of well-deformed nuclei, where the  $\gamma_{K=4}^2$  state is highly anharmonic.

(iii)  $a < 0$ ,  $b = 0$ ,  $c \neq 0$ .

In this case the Hamiltonian (11) is a combination of the quadratic and quadratic-square  $\text{SU}(3)$  Casimir operators. As in the previous case, anharmonicity requires very constrained Hamiltonian parameters once the number of bosons is fixed.

Again, without loss of generality, we fix  $a = -1$ . The energy ratios then read as follows:

$$R_0^{\text{SU}(3)\gamma} = \frac{(4N-3)[2c(4N^2-6N+9)-1]}{(2N-1)(8cN^2+6c-1)}, \quad (18)$$

$$R_4^{\text{SU}(3)\gamma} = \frac{2(2N-3)[4c(2N^2-3N+9)-1]}{(2N-1)(8cN^2+6c-1)}. \quad (19)$$

To keep the energy of the  $\gamma$  excitation positive, the value of  $c$  has the upper limit

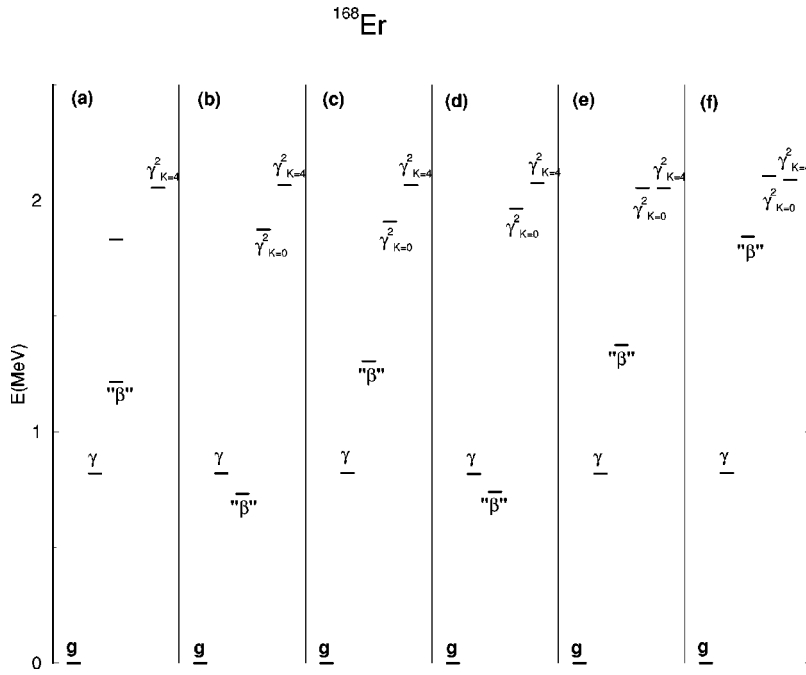


FIG. 9. Band heads of  $^{168}\text{Er}$ . See caption of Fig. 7.

$$c < \frac{1}{8N^2 + 6}. \quad (20)$$

The value  $c = 1/(8N^2 + 6)$  produces a divergence in the two energy ratios and in its neighborhood highly anharmonic behavior is found. In Figs. 4 and 5 are plotted the ratios  $R_0^{\text{SU}(3)\gamma}$  and  $R_4^{\text{SU}(3)\gamma}$ , respectively. Again, for negative values of  $c$ ,  $R_0^{\text{SU}(3)\gamma}$  goes asymptotically to the values 1.45, 1.69, and 1.78 for  $N=5, 10,$  and  $15,$  respectively, while  $R_4^{\text{SU}(3)\gamma}$  goes to 1.33, 1.59, and 1.71. These negative anharmonicities have no phenomenological interest.

In this case the experimental situation can be nicely described. Both  $\gamma_{K=0}^2$  and  $\gamma_{K=4}^2$  states can be accommodated in an anharmonic description. The conclusion is thus that a Hamiltonian with  $\hat{C}_2[\text{SU}(3)]^2$  and  $\hat{C}[\text{SU}(3)]^2$  terms seems to be a good starting point to treat the  $\gamma$  anharmonicity in deformed nuclei.

The description presented here only provides band heads and, to recover a rotational structure, a  $\hat{L}^2$  term must be included. The rotational structure is the same in every band because in the SU(3) limit no mixing exists between rotational and vibrational degrees of freedom. In next subsection these results are illustrated with a schematic calculation for energies and transition probabilities.

#### A schematic application

Let us consider the case of  $^{166}\text{Er}$  which is, as already mentioned, one of particular interest because both double- $\gamma$  excitations (with  $K=0$  and  $K=4$ ) have been identified [8,9]. To carry out the schematic calculation, we use the Hamiltonian (11) with  $b=0$ . The experimental values for the single and double- $\gamma$  energy ratios are  $R_0^\gamma = 2.76$  and  $R_4^\gamma = 2.50$  and can be compared directly with the expressions (18) and (19) leading two values for  $-c/a$ , namely 5

$\times 10^{-4}$  and  $1 \times 10^{-4}$ . Both solutions are fairly close and any value in between them will correctly describe the anharmonicity of the  $K=0$  and  $K=4$  bands. The value of  $a$  and the strength of the rotational term are fixed from the excitation energies of the  $2_1^+$  and  $2_2^+$  levels. After these simple considerations one arrives at the following Hamiltonian:

$$\hat{H} = 13.43 \hat{L} \cdot \hat{L} - 20.84 \hat{C}_2[\text{SU}(3)] + 9.296 \times 10^{-3} \hat{C}_2[\text{SU}(3)]^2, \quad (21)$$

where the coefficients are given in keV. The theoretical and experimental spectra are compared in Fig. 6 and a very good agreement is obtained. However, due to the simplicity of the calculation,  $\gamma$  and  $\beta$  bands are degenerate in energy which is not the case experimentally.

To complete the description,  $E2$  transition probabilities must be computed also. The calculation of  $B(E2)$  values in the SU(3) limit, as in other situations where degeneracies occur, must be treated with care and an appropriate basis must be chosen for states with the same energy. A natural way to do this work is to slightly lift the degeneracy of the SU(3) Hamiltonian. The levels can be split using in the Hamiltonian a value  $\chi = -1.30$  which is very close to its SU(3) value. With this SU(3) breaking the degeneracy is lifted in a natural way because the  $\beta$  band is pushed up in energy, as is observed. One may expect that with this small change in  $\chi$  the SU(3) spectrum will keep its properties. The  $E2$  transition operator is

$$\hat{T}(E2) = e_{\text{eff}} [s^\dagger \tilde{d} + d^\dagger \tilde{s} + \chi (d^\dagger \times \tilde{d})^{(2)}]. \quad (22)$$

The value of  $\chi$  that best reproduces the data is  $\chi = -0.26$ . Note that  $\chi$  in the  $\hat{T}(E2)$  operator and in the Hamiltonian is different. The effective charge is fixed to reproduce

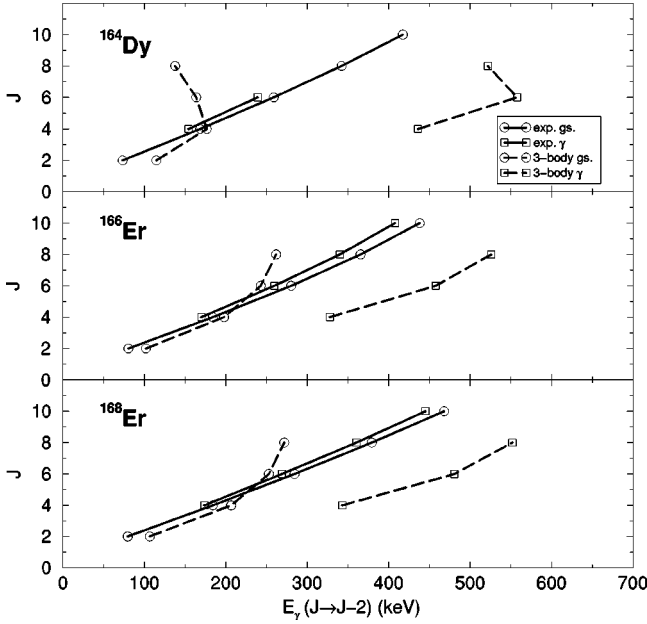


FIG. 10. Total angular momentum  $J$  (dimensionless) of the initial state versus  $\gamma$ -ray energies for  $\Delta J=2$  transitions in ground and  $\gamma$  bands, for  $^{164}\text{Dy}$ ,  $^{166}\text{Er}$ , and  $^{168}\text{Er}$ . Full lines correspond to experimental data and long-dashed lines correspond to the calculated results obtained with the Hamiltonian (9). The corresponding parameters are given in the text.

$B(E2; 2_1^+ \rightarrow 0_1^+)$ :  $e_{\text{eff}}^2 = (1.97)^2$  W.u. In Table I theoretical and experimental transition rates involving the ground and the  $\gamma$  bands are compared.

This simple analysis suggests that a four-body operator of the type in Eq. (21) provides a good description of both single-, and double- $\gamma$  bands. In the next section this schematic analysis is extended to non-SU(3) situations.

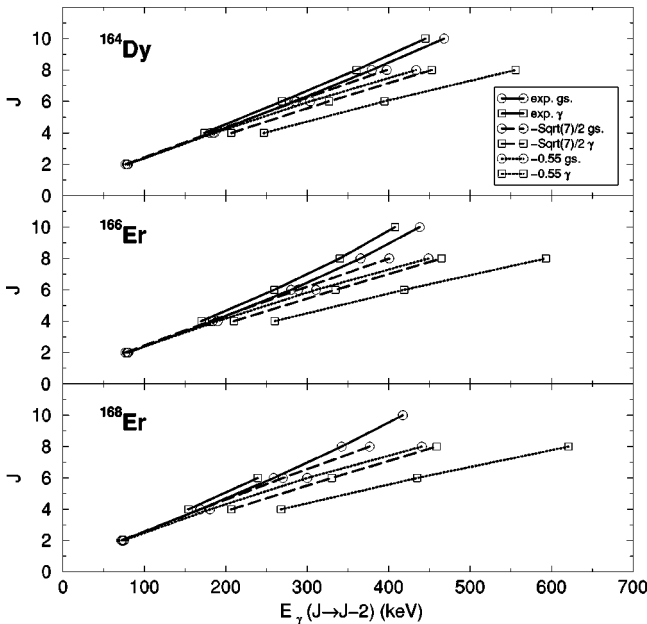


FIG. 11. Same caption as Fig. 10 but calculated results obtained with the Hamiltonian (23).

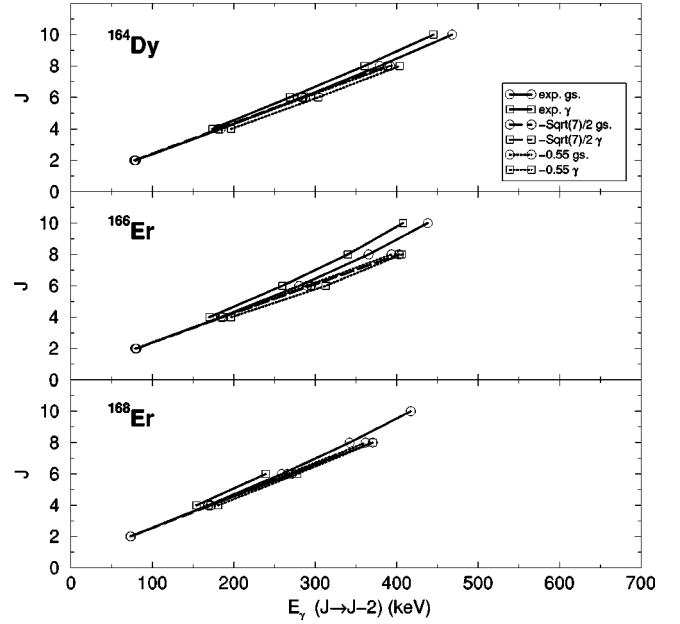


FIG. 12. Same caption as Fig. 10 but calculated results obtained with the Hamiltonian (24).

## V. GENERAL HAMILTONIANS WITH UP TO FOUR-BODY INTERACTIONS

A general Hamiltonian with all possible three- and four-body terms can, in principle, be constructed but the number of parameters is so high that a study, even a schematic one, of the effect of the different terms on energy spectra and electromagnetic transitions is impossible. Schematic IBM Hamiltonians have been used for many years and, in particular, the quadrupole-quadrupole interaction has been very successful in describing a wide variety of nuclear spectra [19,25]. On the other hand, in the previous section it was shown that an expansion in terms of Casimir operators, which are mainly related to quadrupole operators, leads to a satisfactory description of ground, single- and double- $\gamma$  bands. It is worth noting that such an expansion in terms of Casimir operators has been successfully used in molecular physics where spectroscopic data provide many anharmonic states [26]. This leads us to propose a Hamiltonian as a quadrupole expansion that includes up to four-body terms. An alternative Hamiltonian can be based on an expansion in terms of pseudo-Casimir operators, which we define here as operators that become a true Casimir operator only for a particular choice of one structure parameter. For example, the  $\hat{C}_2[\text{SU}(3)]$  operator is related to the quadrupole operator through  $2\hat{Q} \cdot \hat{Q} + \frac{3}{4}\hat{L}^2$  where  $\hat{Q} = s^\dagger \tilde{d} + d^\dagger \tilde{s} \pm \sqrt{7}/2 (d^\dagger \times \tilde{d})^{(2)}$ . If the value  $\pm \sqrt{7}/2$  is changed to  $\chi$ , a new operator  $\hat{C}_2[\text{SU}(3)]_\chi$  is obtained which we refer to as a pseudo-Casimir operator. It is a Casimir operator only for  $\chi = \pm \sqrt{7}/2$ .

Guided by the results of the previous section, two possible Hamiltonians that include up to four-body interactions, can be proposed, one based on a quadrupole expansion and the other on a pseudo-Casimir expansion:



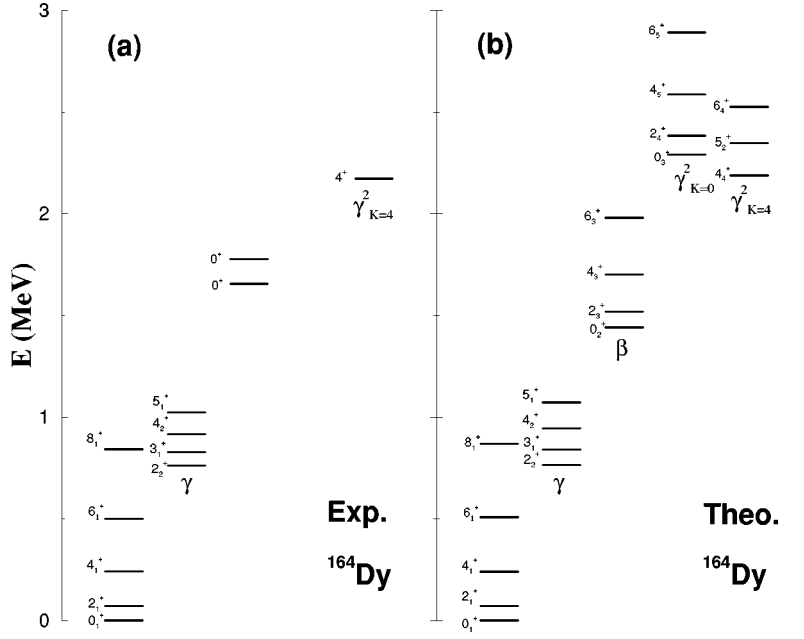


FIG. 13. Experimental (a) and theoretical (b) spectrum for  $^{164}\text{Dy}$ . The Hamiltonian (24) is used with parameters  $\kappa'=12.18$  keV,  $a=-82.90$  keV,  $c=0.05150$  keV, and  $\chi=-0.55$ . The boson number is  $N=16$ .

$$\hat{H}_Q = \kappa' \hat{L} \cdot \hat{L} + a \hat{Q} \cdot \hat{Q} + b (\hat{Q} \times \hat{Q} \times \hat{Q})^{(0)} + c (\hat{Q} \cdot \hat{Q}) (\hat{Q} \cdot \hat{Q}), \quad (23)$$

$$\hat{C}_3[\text{SU}(3)]_\chi = -4\sqrt{35}(\hat{Q}(\chi) \times \hat{Q}(\chi) \times \hat{Q}(\chi))^{(0)} - \frac{9}{2}\sqrt{15}(\hat{L} \times \hat{L} \times \hat{Q}(\chi))^{(0)}. \quad (26)$$

$$\hat{H}_{pc} = \kappa' \hat{L} \cdot \hat{L} + a \hat{C}_2[\text{SU}(3)]_\chi + b \hat{C}_3[\text{SU}(3)]_\chi + c \hat{C}_2[\text{SU}(3)]_\chi^2, \quad (24)$$

For simplicity and taking into account the analysis done in the previous section, in the following  $b=0$  is taken in Eqs. (23) and (24).

where  $\hat{Q} = \hat{Q}(\chi)$  and

$$\hat{C}_2[\text{SU}(3)]_\chi = 2\hat{Q}(\chi) \cdot \hat{Q}(\chi) + \frac{3}{4}\hat{L}^2, \quad (25)$$

#### A. Double- $\gamma$ band heads

There are three nuclei that have double- $\gamma$  bands identified without ambiguity:  $^{164}\text{Dy}$ ,  $^{166}\text{Er}$ , and  $^{168}\text{Er}$  [7–10]. In this section the band heads of these nuclei are studied using the

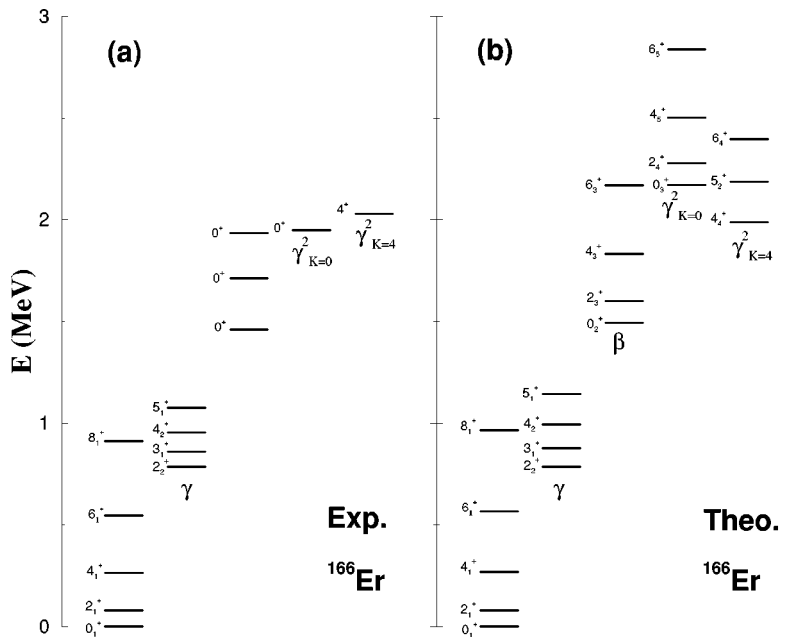


FIG. 14. Experimental (a) and theoretical (b) spectrum for  $^{166}\text{Er}$ . The Hamiltonian (24) is used with parameters  $\kappa'=13.55$  keV,  $a=-75.40$  keV,  $c=0.05286$  keV, and  $\chi=-0.45$ . The boson number is  $N=15$ .

Hamiltonians (23) and (24) to get an improved description of the anharmonicity phenomenon.

The number of bosons for  $^{164}\text{Dy}$  and  $^{168}\text{Er}$  is  $N=16$  while for  $^{166}\text{Er}$  it is  $N=15$ . In the different calculations shown in this section the parameters of the Hamiltonian have been chosen as to reproduce as well as possible not only the heads of single- and double- $\gamma$  bands but also the structure of the bands. Because these calculations are schematic and do not try to be the best answer, the parameters of the Hamiltonian, for simplicity, will not be given fully and only in the case of final spectra will be shown. For comparison, the calculation with three-body terms (see Sec. III and Ref. [24]) is also included.

In Figs. 7–9 the heads of single- and double-phonon bands are shown. In each figure six panels are included: (a) experimental data, (b) calculation with Hamiltonian (23) and  $\chi = -\sqrt{7}/2$ , (c) calculation with Hamiltonian (23) and  $\chi = -0.55$ , (d) calculation with Hamiltonian (24) and  $\chi = -\sqrt{7}/2$ , (e) calculation with Hamiltonian (24) and  $\chi = -0.55$ , and (f) calculation with a three-body term  $(d^\dagger \times d^\dagger \times d^\dagger)^{(4)} \cdot (\tilde{d} \times \tilde{d} \times \tilde{d})^{(4)}$ . In each panel, from left to right are represented the ground state, the  $\gamma$  band head, the  $\beta$  band head, the double- $\gamma$   $K=0$  band head, and the double- $\gamma$   $K=4$  band head. Due to the controversy on the nature of the  $\beta$  band, several candidates for the latter have been included. For the same reason in the figures will be used the label ‘‘ $\beta$ .’’ In  $^{164}\text{Dy}$  and  $^{168}\text{Er}$  no information on the double- $\gamma$   $K=0$  band exists. The value  $\chi = -0.55$  is chosen as an alternative to the SU(3) value because it describes very well the  $E2$  transition probabilities in this mass region. Also, the same value of  $\chi$  is taken in the Hamiltonian and in the transition operator, in line with the consistent- $Q$  formalism (CQF) [27]. In Sec. V C this ansatz is used in the complete analysis of spectra and  $B(E2)$  transitions for  $^{164}\text{Dy}$ ,  $^{166}\text{Er}$ , and  $^{168}\text{Er}$ .

The most striking feature of Figs. 7–9 is that in all calculations the position of the double- $\gamma$  band heads and the degree of anharmonicity is well reproduced. Thus the energies of the different band heads only are not sufficient to completely determine the Hamiltonian. Nevertheless, not all possible terms are able to create sufficient anharmonicity in the double- $\gamma$  bands. For example, in the case of three-body terms, a phenomenological study of the most relevant type of term shows that only  $(d^\dagger \times d^\dagger \times d^\dagger)^{(4)} \cdot (\tilde{d} \times \tilde{d} \times \tilde{d})^{(4)}$  is able to produce the required anharmonicity (see Sec. III and Ref. [24]). On the other hand, only a few four-body interactions have been explored here and it cannot be excluded that other four-body terms can produce the appropriate degree of anharmonicity.

In order to decide which Hamiltonian is more appropriate, a description should be attempted not only of band heads but also of the structure of the bands and of  $E2$  transition probabilities.

### B. Moments of inertia

The study of the moments of inertia of the lowest bands is a very sensitive way to test the different calculations shown in Figs. 7–9. Particular attention will be paid to the dynamic

moment of inertia which can be obtained from the relation between angular momentum and  $\gamma$ -ray energy [28,29] and can be approximated by

$$\mathcal{I} \approx 2\hbar^2 \frac{dJ}{dE_\gamma}, \quad (27)$$

where  $J$  is given dimensionless. In a plot of  $\gamma$ -ray energy versus  $J$ ,  $\mathcal{I}$  will be the slope. Equation (27) can be used to study the structure of the rotational bands in comparison with experimental results.

In Fig. 10 the moments of inertia of the ground and  $\gamma$  bands in the nuclei  $^{164}\text{Dy}$ ,  $^{166}\text{Er}$ , and  $^{168}\text{Er}$  are compared to those obtained with the Hamiltonian of Sec. III. The parameters for  $^{164}\text{Dy}$  are  $\kappa = 24.2$  keV,  $\chi = -0.55$ ,  $\kappa' = -6.0$  keV, and  $\theta_4 = 51.0$  keV, for  $^{166}\text{Er}$  are indicated in Sec. III and for  $^{168}\text{Er}$  are  $\kappa = 24.1$  keV,  $\chi = -0.55$ ,  $\kappa' = -1.9$  keV, and  $\theta_4 = 31.6$  keV. The predicted moments of inertia disagree completely with the almost pure rotational structure observed experimentally. So, although this simple description based on one single three-body term describes well the anharmonic position of the double-phonon band heads, it fails in the moments of inertia of ground and  $\gamma$  bands. A more realistic description needs others three-body terms. A recent analysis [23] shows, however, that Hamiltonians with *two* different three-body terms cannot get the correct moment of inertia.

The results with the Hamiltonian (23) are shown in Fig. 11. Two different calculations are shown which correspond to panels *b* and *c*, respectively, of Figs. 7–9. In this case a better agreement is obtained but still some discrepancies remain, especially when a realistic value for  $\chi$  is taken ( $\chi = -0.55$ ). Finally, in Fig. 12 the results with the Hamiltonian (24) are compared with the data. Again, two different calculations are shown which correspond to panels *d* and *e*, respectively, of Figs. 7–9. Here, good agreement is found both for  $\chi = -\sqrt{7}/2$  and  $\chi = -0.55$ .

The different results with the Hamiltonians (23) and (24), can be understood qualitatively by analyzing the structure of  $[\hat{Q}(\chi) \cdot \hat{Q}(\chi)][\hat{Q}(\chi) \cdot \hat{Q}(\chi)]$ . With just two-body terms the Hamiltonians (23) and (24) are equivalent. This is different when up to four-body terms are included because  $[\hat{Q}(\chi) \cdot \hat{Q}(\chi)][\hat{Q}(\chi) \cdot \hat{Q}(\chi)]$  does not only contribute to  $\hat{C}_2[\text{SU}(3)]_\chi^2$  and  $\hat{L}^2$  but also to  $(\hat{L}^2)^2$ . This can be clarified with the equation

$$\begin{aligned} & [\hat{Q}(\chi) \cdot \hat{Q}(\chi)][\hat{Q}(\chi) \cdot \hat{Q}(\chi)] \\ &= \frac{1}{4} \hat{C}_2[\text{SU}(3)]_\chi^2 - \frac{3}{8} \hat{C}_2[\text{SU}(3)]_\chi^2 \hat{L}^2 + \frac{9}{64} (\hat{L}^2)^2. \end{aligned} \quad (28)$$

As a consequence,  $[\hat{Q}(\chi) \cdot \hat{Q}(\chi)][\hat{Q}(\chi) \cdot \hat{Q}(\chi)]$  substantially modifies the rotational structure of a band even in the case of pure SU(3). This is how it can be qualitatively understood that *a description in terms of pseudo-Casimir operators is the most appropriate for dealing with anharmonic*

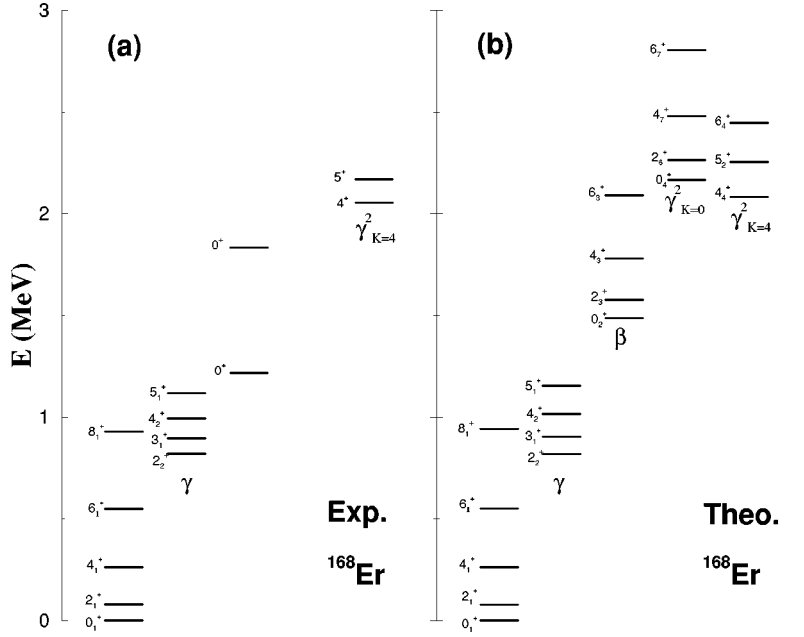


FIG. 15. Experimental (a) and theoretical (b) spectrum for  $^{168}\text{Er}$ . The Hamiltonian (24) is used with parameters  $\kappa' = 13.23$  keV,  $a = -67.25$  keV,  $c = 0.04080$  keV, and  $\chi = -0.50$ . The boson number is  $N = 16$ .

vibrations. In the next section a complete analysis is given of the nuclei under study in the framework of CQF using the Hamiltonian (24).

### C. Realistic calculations

The complete calculated spectra of  $^{164}\text{Dy}$ ,  $^{166}\text{Er}$ , and  $^{168}\text{Er}$  and the most relevant  $E2$  transition probabilities are presented in this section. They are compared with existing data. In each calculation the same value of  $\chi$  has been used both in the Hamiltonian (24) and in the electromagnetic operator (22). Finally, the effective charge in the transition operator (22),  $e_{\text{eff}}$ , was fixed for each nucleus to reproduce the  $B(E2; 2_1^+ \rightarrow 0_1^+)$  value.

The experimental and calculated spectra for  $^{164}\text{Dy}$ ,  $^{166}\text{Er}$ , and  $^{168}\text{Er}$  are shown in Figs. 13–15, respectively. The parameters used in the calculations are listed in Table II. The parameters that yield the best fit to the energy spectra are very similar in the three cases which is consistent with the analysis carried out in the preceding sections. The overall description of the energies is satisfactory. The calculated low-lying bands are in good agreement with their experimental counterparts (see also Fig. 12) while the double- $\gamma$  bandhead energies are close to the experimental values. The calculated ratios (8) are:  $R_0^\gamma = 3.31$  and  $R_4^\gamma = 2.81$  for  $^{164}\text{Dy}$ ,  $R_0^\gamma = 3.08$  and  $R_4^\gamma = 2.43$  for  $^{166}\text{Er}$ , and  $R_0^\gamma = 2.93$  and  $R_4^\gamma = 2.46$  for  $^{168}\text{Er}$ , to be compared with the experimental ones:

TABLE II. Parameters of the Hamiltonian (24) obtained in the best fit to spectra and  $B(E2)$  transitions in the nuclei  $^{164}\text{Dy}$ ,  $^{166}\text{Er}$ , and  $^{168}\text{Er}$ .

Nucleus	$\kappa'$ (keV)	$a$ (keV)	$c$ (keV)	$\chi$	$N$
$^{164}\text{Dy}$	12.18	-82.90	0.05150	-0.55	16
$^{166}\text{Er}$	13.55	-75.40	0.05286	-0.45	15
$^{168}\text{Er}$	13.23	-67.25	0.04080	-0.50	16

$R_4^\gamma = 2.84$  for  $^{164}\text{Dy}$ ,  $R_0^\gamma = 2.82$  and  $R_4^\gamma = 2.45$  for  $^{166}\text{Er}$ , and  $R_4^\gamma = 2.50$  for  $^{168}\text{Er}$ . Only for the  $\gamma_{K=0}^2$  vibration the experimental and theoretical results are slightly different in the sense that this framework overestimates the anharmonic behavior for the  $\gamma_{K=0}^2$  band. This can be corrected by increasing the value of  $|\chi|$  in the Hamiltonian which, however, will introduce one more parameter because in the electromagnetic operator a different value of  $\chi$  must be used.

For the calculation of  $E2$  transition probabilities the same  $\chi$  values as in the Hamiltonian are adopted. The effective charges are  $e_{\text{eff}}^2 = (1.66)^2$  W.u.,  $e_{\text{eff}}^2 = (1.83)^2$  W.u., and  $e_{\text{eff}}^2 = (1.67)^2$  W.u., for  $^{164}\text{Dy}$ ,  $^{166}\text{Er}$ , and  $^{168}\text{Er}$ , respectively. In Tables III–V the observed  $B(E2)$  values and ratios concerning  $\gamma$ -vibrational states are compared with the theoretical results. In general, a good overall agreement is obtained in the three cases under study.

## VI. CONCLUSIONS

In this paper the problem of anharmonicity in the  $\beta$  and  $\gamma$  vibrations of deformed nuclei was addressed in the context

TABLE III. Observed and calculated  $B(E2)$  values and ratios for  $^{164}\text{Dy}$ . The  $E2$  operator (22) is used with  $e_{\text{eff}}^2 = (1.66)^2$  W.u. and  $\chi = -0.55$ .

	$B(E2)$ value or ratio	
	Observed	Calculated
$B(E2; 2_1^+ \rightarrow 0_1^+)$ (W.u.)	$209 \pm 3^a$	209
$B(E2; 4_1^+ \rightarrow 2_1^+)$ (W.u.)	$272 \pm 14^a$	298
$B(E2; 2_\gamma^+ \rightarrow 0_1^+)$ (W.u.)	$4.0 \pm 0.4^a$	3.9
$B(E2; 4_{\gamma\gamma}^+ \rightarrow 2_\gamma^+)$	$0.5 - 3.9^b$	3.3
$B(E2; 2_\gamma^+ \rightarrow 0_1^+)$		

<sup>a</sup>From Ref. [31].

<sup>b</sup>From Ref. [7].

TABLE IV. Observed and calculated  $B(E2)$  values and ratios for  $^{166}\text{Er}$ . The  $E2$  operator (22) is used with  $e_{\text{eff}}^2 = (1.83)^2$  W.u. and  $\chi = -0.45$ .

	$B(E2)$ value or ratio	
	Observed	Calculated
$B(E2; 2_1^+ \rightarrow 0_1^+)$ (W.u.)	$214 \pm 10^a$	214
$B(E2; 4_1^+ \rightarrow 2_1^+)$ (W.u.)	$311 \pm 10^a$	304
$B(E2; 2_\gamma^+ \rightarrow 0_1^+)$ (W.u.)	$5.5 \pm 0.4^a$	5.9
$B(E2; 0_{\gamma\gamma}^+ \rightarrow 2_\gamma^+)$	$3.8 \pm 1.3^b$ ( $2.2_{-0.7}^{+1.1}$ $^c$ )	1.8
$B(E2; 2_\gamma^+ \rightarrow 0_1^+)$		
$B(E2; 4_{\gamma\gamma}^+ \rightarrow 2_\gamma^+)$	$1.3 \pm 0.4^b$ ( $0.9 \pm 0.3$ $^c$ )	2.7
$B(E2; 2_\gamma^+ \rightarrow 0_1^+)$		

<sup>a</sup>From Ref. [30].

<sup>b</sup>From Ref. [9].

<sup>c</sup>From Ref. [8].

of the interacting boson model. The occurrence or not of anharmonicity was shown to be related to the order of the interactions between the bosons and the conclusions of the analysis can be summarized as follows. If the Hamiltonian includes up to two-body interactions, no sizable anharmonicity can be obtained and the observed behavior cannot be obtained. The origin of this behavior is related to the existence of a first-order phase transition between rotational and vibrational nuclei [19] which excludes any interplay between one- and two-body terms, necessary to obtain anharmonic spectra. For up to three-body interactions that preserve SU(3) symmetry it can be *shown* that the observed anharmonicity cannot be fully reproduced. Furthermore, extensive numerical calculations indicate that even a general IBM Hamiltonian that includes up to three-body interactions has difficulty in reproducing all observed aspects of ground, single- and double- $\gamma$  bands. However, due to the large parameter space of three-body interactions which is difficult to search exhaustively, this cannot be considered as a firm conclusion and alternative approaches (e.g., mean-field) should be tried to tackle the same problem. Finally, it was shown that a simple parametrization of the IBM Hamiltonian that includes up to four-body interactions can account for all observed properties of the three deformed nuclei with firmly established double- $\gamma$  vibrations. In particular, the introduction of

TABLE V. Observed and calculated  $B(E2)$  values and ratios for  $^{168}\text{Er}$ . The  $E2$  operator (22) is used with  $e_{\text{eff}}^2 = (1.67)^2$  W.u. and  $\chi = -0.50$ .

	$B(E2)$ value or ratio	
	Observed	Calculated
$B(E2; 2_1^+ \rightarrow 0_1^+)$ (W.u.)	$207 \pm 10^a$	207
$B(E2; 4_1^+ \rightarrow 2_1^+)$ (W.u.)	$318 \pm 10^a$	294
$B(E2; 2_\gamma^+ \rightarrow 0_1^+)$ (W.u.)	$4.80 \pm 0.17^a$	4.6
$B(E2; 4_{\gamma\gamma}^+ \rightarrow 2_\gamma^+)$	$0.5 - 1.6^b$	2.7
$B(E2; 2_\gamma^+ \rightarrow 0_1^+)$		
$B(E2; 5_{\gamma\gamma}^+ \rightarrow 3_\gamma^+)$	$0.7 - 3.5^b$	2.1
$B(E2; 2_\gamma^+ \rightarrow 0_1^+)$		

<sup>a</sup>From Ref. [32].

<sup>b</sup>From Ref. [10].

SU(3) pseudo-Casimir operators allows to describe the double-phonon states while keeping correct the properties of low-lying bands.

It should be emphasized that, in spite of its fourth-order character, the Hamiltonian considered here is only slightly more complex than the usual IBM Hamiltonian (one more parameter) and is a straightforward extension of the consistent- $Q$  formalism that was previously successfully applied to many nuclei. Also clear from our study is the need for more experimental information about the double-phonon vibrations in deformed nuclei beyond the three cases known at present: our analysis indeed has shown that this information represents a challenging test of any theoretical description of deformed nuclei.

## ACKNOWLEDGMENTS

We are grateful to C. E. Alonso, K. Heyde, and F. Iachello for valuable comments. Two of the authors (P.V.I. and J.E.G.R.) wish to thank the Institute for Nuclear Theory, University of Washington, where this work was initiated. One of the authors (J.E.G.R.) thanks the FWO for financial support. This work was supported in part by the Spanish DGICYT under Project No. PB98-1111. J.E.G.R. thanks the Fund of Scientific Research, Flanders, Belgium for financial support.

- [1] A. Bohr and B. Mottelson, *Nuclear Structure. II Nuclear Deformations* (Benjamin, Reading, MA, 1975).
- [2] P. E. Garret, M. Kadi, C. A. McGrath, V. Sorokin, M. Li, M. Yeh, and S. W. Yates, Phys. Lett. B **400**, 250 (1997).
- [3] C. Fahlander *et al.*, Nucl. Phys. **A485**, 327 (1988).
- [4] T. Belgya, G. Molnár, and S. W. Yates, Nucl. Phys. **A607**, 43 (1996).
- [5] H. G. Börner and J. Jolie, J. Phys. G **19**, 217 (1993).
- [6] D. D. Burke, Phys. Rev. Lett. **73**, 1899 (1994).
- [7] F. Corminbeuf, J. Jolie, H. Lehmann, K. Fohl, F. Hoyler, H. G. Börner, C. Doll, and P. E. Garrett, Phys. Rev. C **56**, R1201 (1997).

- [8] C. Fahlander, A. Axelsson, M. Heinebrodt, T. Härtlein, and D. Schwalm, Phys. Lett. B **388**, 475 (1996).
- [9] P. E. Garrett *et al.*, Phys. Rev. Lett. **78**, 4545 (1997).
- [10] H. G. Börner, J. Jolie, S. J. Robinson, B. Krusche, R. Piepenbring, R. F. Casten, A. Aprahamian, and J. P. Draayer, Phys. Rev. Lett. **66**, 691 (1991).
- [11] V. G. Soloviev, A. V. Sushkov, and N. Yu Shirikova, J. Phys. G **20**, 113 (1994).
- [12] V. G. Soloviev, A. V. Sushkov, and N. Yu Shirikova, Phys. Rev. C **51**, 551 (1995).
- [13] A. Bohr and B. R. Mottelson, Phys. Scr. **25**, 28 (1982).

- [14] M. K. Jammari and R. Piepenbring, Nucl. Phys. **A487**, 77 (1988).
- [15] M. Matsuo and K. Matsuyanagi, Prog. Theor. Phys. **76**, 93 (1986).
- [16] M. Matsuo and K. Matsuyanagi, Prog. Theor. Phys. **78**, 591 (1987).
- [17] N. Yoshinaga, Y. Akiyama, and A. Arima, Phys. Rev. Lett. **56**, 1116 (1986).
- [18] N. Yoshinaga, Y. Akiyama, and A. Arima, Phys. Rev. C **38**, 419 (1988).
- [19] F. Iachello and A. Arima, *The Interacting Boson Model* (Cambridge University Press, Cambridge, 1987).
- [20] J. E. García-Ramos, C. E. Alonso, J. M. Arias, P. Van Isacker, and A. Vitturi, Nucl. Phys. **A637**, 529 (1998).
- [21] F. Iachello, N. V. Zamfir, and R. F. Casten, Phys. Rev. Lett. **81**, 1191 (1998).
- [22] P. Van Isacker and J. Q. Chen, Phys. Rev. C **24**, 684 (1981).
- [23] J.E. García-Ramos (unpublished).
- [24] J. E. García-Ramos, C. E. Alonso, J. M. Arias, and P. Van Isacker, Phys. Rev. C **61**, 047305 (2000).
- [25] R. F. Casten and D. D. Warner, Rev. Mod. Phys. **60**, 389 (1988).
- [26] F. Iachello and R. D. Levine, *Algebraic Theory of Molecules* (Oxford University Press, New York, 1995).
- [27] D. D. Warner and R. F. Casten, Phys. Rev. Lett. **48**, 1385 (1982).
- [28] X. Wu, A. Aprahamian, J. Castro-Ceron, and C. Baktash, Phys. Lett. B **316**, 235 (1993).
- [29] H. Ejiri and M. J. A. De Voigt, *Gamma-ray and Electron Spectroscopy in Nuclear Physics* (Clarendon, Oxford, 1989).
- [30] E. N. Shurshikov and N. V. Timofeeva, Nucl. Data Sheets **67**, 45 (1992).
- [31] E. N. Shurshikov and N. V. Timofeeva, Nucl. Data Sheets **65**, 365 (1992).
- [32] V. S. Shirley, Nucl. Data Sheets **71**, 261 (1994).